

**Molecular Cell, Volume 53**

**Supplemental Information**

**A Feedforward Regulatory Loop between HuR and the Long Noncoding RNA linc-MD1 Controls Early Phases of Myogenesis**

Ivano Legnini, Mariangela Morlando, Arianna Mangiavacchi, Alessandro Fatica, and Irene Bozzoni

**Figure S1**

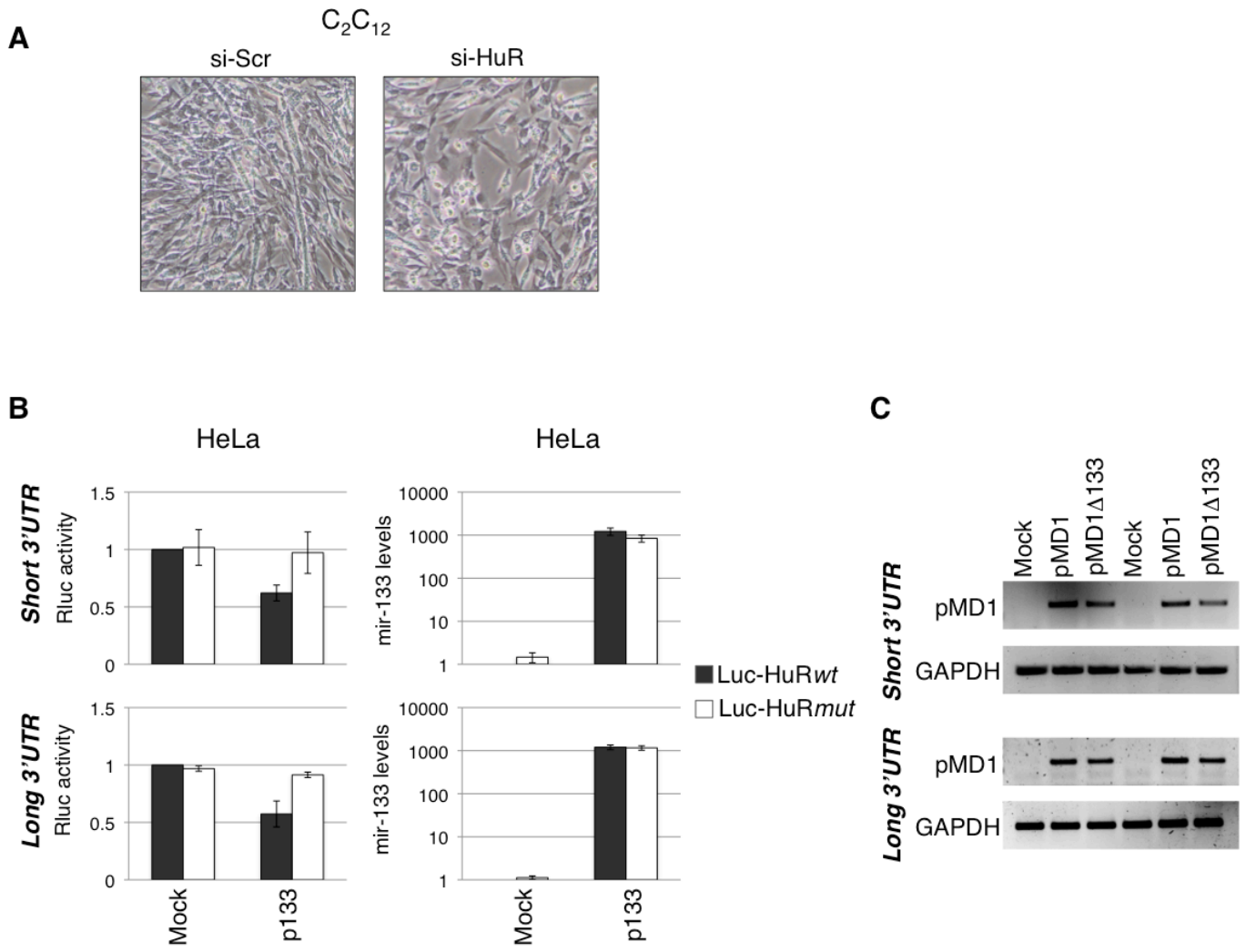


**Figure S2**

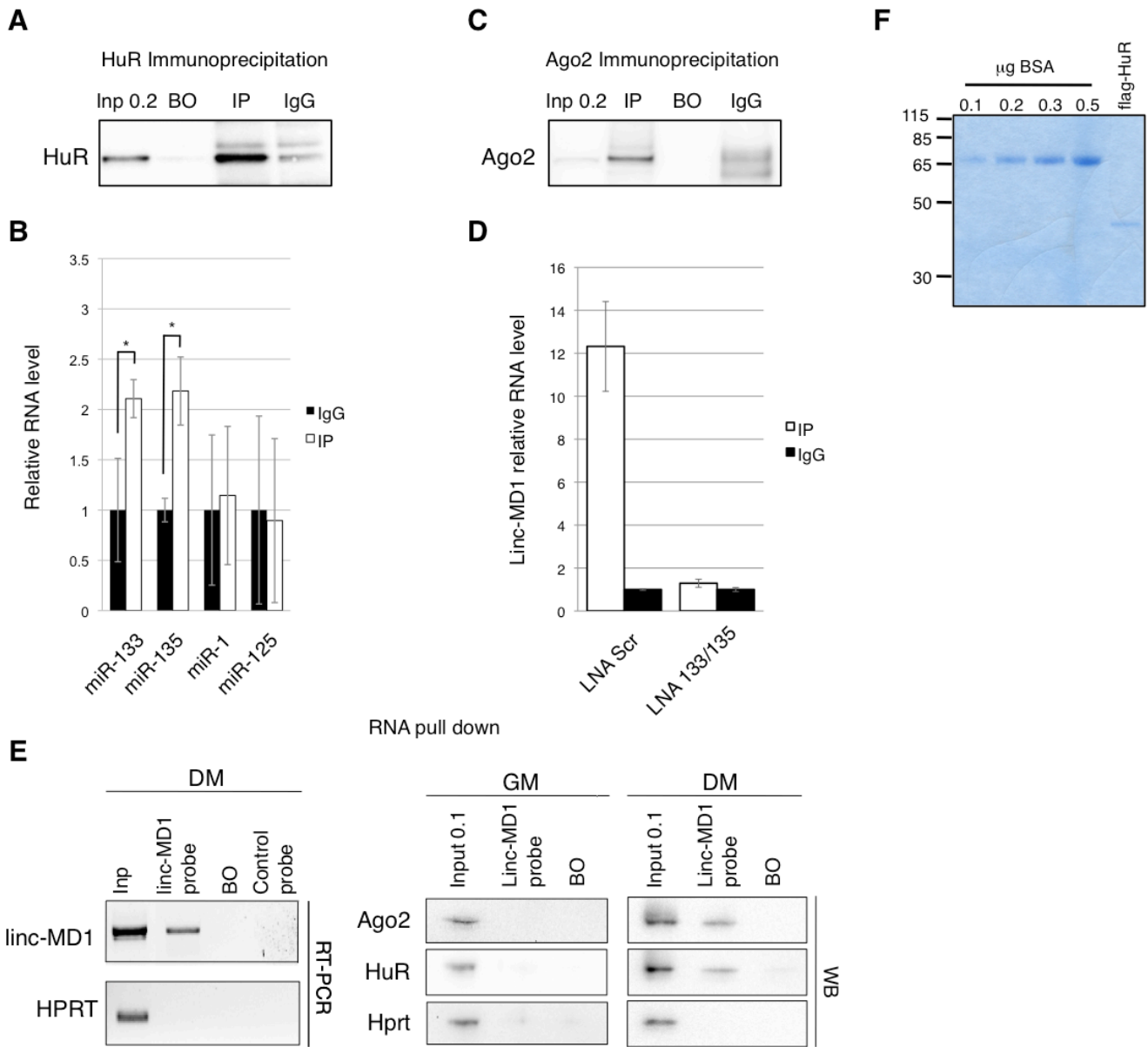
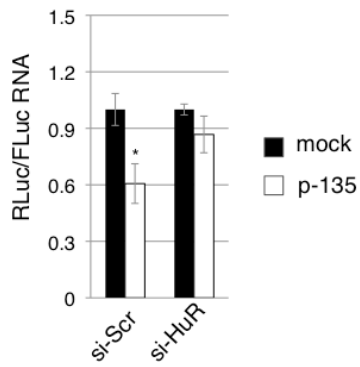


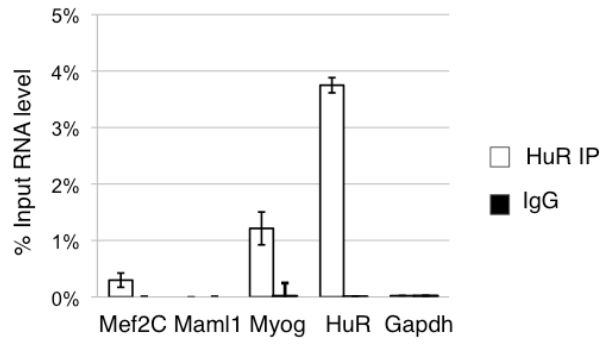


**Figure S4**

**A**



**B**

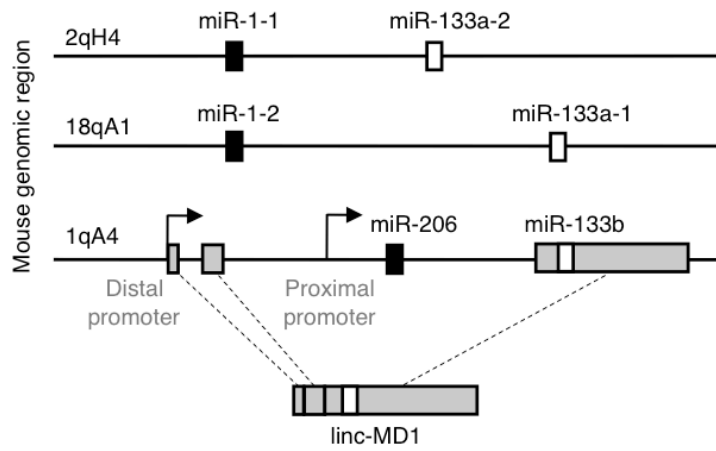


**C**

**mmu-miR-133a/b reads**

	All reads available (74 exp.)	Skeletal Muscle (GSM5398 75)
<b>133a</b>	205,823	1,350
<b>133b</b>	46,195	26

**D**



## Supplemental Figures Legends

### Figure S1, related to Figure 1. Role of HuR in differentiation and its control by miR-133

A. C<sub>2</sub>C<sub>12</sub> cells differentiated for 48 hours and treated either with control (si Scr) or anti HuR (si HuR) siRNAs. Images were taken with a Zeiss Axio Observer A1 microscope at 10X magnification.

B. Left panels: luciferase activity of short and long Luc-HuR<sup>wt</sup> and mutant derivatives co-transfected in HeLa cells together with a control plasmid (Mock) or with a plasmid expressing miR-133 (p-133). FLuc/RLuc RQ is shown with respect to a control sample set to a value of 1. Right panels: Graphs showing the levels of miR-133 in the samples treated as in left panels, measured by qRT-PCR. Data were derived from at least three independent experiments; error bars represents standard error.

C. Levels of pMD1 and pMD1 $\Delta$ 133 in samples treated as in Fig. 1C, measured by RT-PCR. GAPDH is used as control.

### Figure S2, related to Figure 2. RNA and protein interactions with linc-MD1

A. Western blot analysis of the HuR RIP experiment of Figure 2A showing the presence of HuR in the IP sample with respect to BO and IgG samples.

B. Graph showing the enrichment of miR-133 and miR-135, measured by qRT-PCR, in the IP (white bars) and IgG (black bars) samples of the experiment of Figure 2A. miR-1 and miR-125 are used as negative controls. Error bars represent standard errors based on three independent experiments. One asterisk correspond to p<0.05.

C. Western blot analysis of the Ago RIP experiment of Figure 2B showing the presence of Ago in the IP sample with respect to BO and IgG samples.

D. The graph shows the enrichment of linc-MD1 in the IP (black bars) with respect to IgG (white bars) samples from Ago-RIP experiment performed in differentiating C<sub>2</sub>C<sub>12</sub> cells treated with control (LNA-Scr) or anti-miR-133/135 (LNA-133/135) LNA oligonucleotides.

E. Left panels: RT-PCR analysis showing that linc-MD1 is present in the *bound* fraction of the RNA-pull down experiment shown in Figure 2C, but not in the beads only (BO) and unspecific RNA control (Control probe) samples. HPRT is used as negative control. Right panels: Western Blot analysis showing Ago2, HuR and Hprt proteins in linc-MD1 pull down performed in GM versus DM cultured C<sub>2</sub>C<sub>12</sub> cells.

F. Coomassie staining showing the quality of the purified flag-HUR protein. Different amounts of BSA are used as a control of quantity. Markers of molecular weight are also shown.

### Figure S3, related to Figure 3. Effects of HuR on linc-MD1 processing

A. Same cellular equivalents of nuclear (Nuc) and cytoplasmic (Cyt) protein extracts from C<sub>2</sub>C<sub>12</sub> cells, differentiated for the indicated time points, were analysed by Western blot analysis using anti-HuR antibody. Hprt is used as loading control as well as a control for contamination between the nuclear and cytoplasmic fractions.

B. Schematic representation indicating the species deriving from the linc-MD1 locus and the oligo used for their detection by RT-PCR.

C. qRT-PCR analysis on RNA from HeLa cells transfected with p133a, p133b or empty vector (negative control). cDNA was prepared using Exiqon miRCURY cDNA synthesis kit and analyzed with LNA probes targeting miR-133a or miR-133b (black and white bars respectively). qRT-PCR was performed on pure cDNAs and mixed ones made of 25% of miR-133a, 50% of both or 25% miR-133b.

D. Graph showing the 133b/133a reads ratio measured by small RNA-seq on RNA samples obtained from differentiating C<sub>2</sub>C<sub>12</sub> cells treated with control (si-Scr) and anti HuR (si-HuR) siRNAs. A general decrease of reads was obtained in the absence of HuR, probably reflecting the effect of HuR on transcriptional factors such as MyoD, Myog, p21. Nevertheless, in these conditions, the decrease of miR-133b results lower than that of its paralogue miR-133a. MiRNA

reads are available as a separate spreadsheet named “smallnaseq”.

E. RT-PCR showing the level of linc-MD1 in differentiating C2C12 cells upon 10ng/ml leptomycin B (LMB) treatment . GAPDH is used as control.

F. miR-133b levels measured by qRT-PCR performed on cDNA prepared with Qiagen miScript system using RNA from HeLa cells treated with an empty vector (p-, white bars) and an HuR overexpressing vector (pHuR, black bars) in combination either with a linc-MD1 expressing vector (pMD1*wt*) or its mutant derivative lacking the HuR binding site (pMD1 $\Delta$ HuR). miR-133b levels normalized to U6snRNA are set to 1 in the p- samples. Error bars represent standard error from 3 independent experiments.

G. Western blot analysis showing the level of the HuR protein in the nuclear fractions from HeLa cells upon HuR depletion. Actinin is used as loading control.

H. *in vitro* processing with <sup>32</sup>P-UTP labelled pri-miR-133b and pri-miR-9-2, with nuclear extracts from HeLa cells treated with control (si Scr) and anti HUR (si HuR) siRNAs. Samples with no extract (mock) were used as control. The pre-miR-133b and pre-miR-9-2 are indicated as well as a panel with a magnification of higher exposition for pre-miR-133b visualization. The asterisk indicates a pri-miR-9-2 unspecific cleavage. The experiment has been performed two times.

I. Putative structure of the pri-miR-133b stem-loop. The mature miR-133b sequence is shown in bold. Arrows indicate the positions of the Drosha cleavage sites.

#### **Figure S4, related to Figure 4. Cytoplasmic role of HuR**

A. q-RT-PCR for Luc-MD1*wt* expression in condition of HuR depletion (si-HuR) versus control treated cells (si-Scr), combined with overexpression of miR-135 (p-135) versus mock-treated cells (psp). Bars represent RLuc/FLuc mRNA RQ. Error bars represents standard error while the asterisk corresponds to two tailed Student t test  $p < 0.05$ .

B. HuR RNP immunoprecipitation followed by qRT-PCR analysis performed on differentiated C<sub>2</sub>C<sub>12</sub> cells showing % of input RNA recovered in IP (white bars) and IgG (black bars) for MEF2C and MAML1 with respect to positive controls (Myogenin and HuR mRNAs) and the negative control GAPDH mRNA.

C. NGS data analysis showing the reads available for miR-133a and miR-133b. Reads were obtained from mirbase database (Kazomara et al., 2011).

D. Schematic representation indicating the genomic position and organization of the three genomic loci coding for miR-133 in mouse.

**Table S1, related to Figure 1. – Predicted top 20 target mRNAs for miR-133 and miR-135 according to Miranda, filtered for expression in skeletal muscle.**

<b>miR-133 top 20 predicted targetes</b>			<b>miR-135 top 20 predicted targets</b>		
Associated Gene Name	Ensembl Gene ID	score	Associated Gene Name	Ensembl Gene ID	score
Xirp1	ENSMUSG00000079243	443	Zbtb20	ENSMUSG00000022708	1154
Nfic	ENSMUSG00000055053	438	Lpp	ENSMUSG00000033306	738
Ahcy11	ENSMUSG00000027893	436	Hnrnpa3	ENSMUSG00000059005	731
Purb	ENSMUSG00000094483	427	Gpr116	ENSMUSG00000056492	722
Zbtb20	ENSMUSG00000022708	420	Celf2	ENSMUSG00000002107	711
Pum2	ENSMUSG00000020594	326	Zyg11b	ENSMUSG00000034636	618
Celf1	ENSMUSG00000005506	308	Arl5a	ENSMUSG00000036093	610
St3gal6	ENSMUSG00000022747	305	Tnpo1	ENSMUSG00000009470	605
Mrpl11	ENSMUSG00000024902	303	Clcn5	ENSMUSG00000004317	596
Shisa5	ENSMUSG00000025647	302	Fyco1	ENSMUSG00000025241	596
Pnpla2	ENSMUSG00000025509	299	Ncoa4	ENSMUSG00000056234	593
Usp7	ENSMUSG00000022710	294	Purb	ENSMUSG00000094483	592
Mllt3	ENSMUSG00000028496	294	Eif4g2	ENSMUSG00000005610	590
Aars	ENSMUSG00000031960	294	Foxn3	ENSMUSG00000033713	588
Arhgef12	ENSMUSG00000059495	294	Cxcl12	ENSMUSG00000061353	588
Lhfp	ENSMUSG00000048332	291	Tnrc6b	ENSMUSG00000047888	583



Crk	ENSMUSG00000017776	290	Stradb	ENSMUSG00000026027	582
Slc30a9	ENSMUSG00000029221	290	Mapre1	ENSMUSG00000040430	580
<b>Elavl1</b>	<b>ENSMUSG00000040028</b>	<b>290</b>	Setd7	ENSMUSG00000027479	576
Zc3h14	ENSMUSG00000021012	288	Pitpnc1	ENSMUSG00000037111	572

**Table S2, related to Experimental Procedures. - Oligonucleotides used in this study**

<b>Luciferase constructs</b>	sequence
HUR 3'UTR-S NOT1 fw	ATTGCGGCCGCCTCAGTCCAGCTCTATAGTGTTG
HUR 3'UTR-S NOT1 rev	ATTGCGGCCGCCAGAACAGAACCCCAAACG
HUR 3'UTR-L NOT1 rev	ATTGCGGCCGCCTTGGCACATTACCTAGAAGTTTC
HUR 3'UTR D133 1° rev	GCAGCTCCAGTATATTCCAG
HUR 3'UTR D133 1st fw	GTTCTCATTGGTGCCTGGGC
HUR 3'UTR D133 2° fw	G TTCAGGCCCTATAGGCTGG
HUR 3'UTR D133 2° rev	TGGAGGTGGGATTCTCCTCAG
<b>RT-PCR</b>	
Total linc-MD1 fw	GCAAGAAAACCACAGAGGAGG
Total linc-MD1 rev	GTGAAGTCCTTGGAGTTTGAGCA
Uncleaved linc-MD1 fw	CTCTTTGCAGTGGGACAGCT
Uncleaved linc-MD1 rev	TGTGAACTTGGGCTTTCTCC
linc-hMD1 fw	AGGCATAGAAATGCGAACCA
linc-hMD1 rev	ATTGTCAGAAATAAAGACTC
GAPDH fw	TGACGTGCCGCCTGGAGAAA
GAPDH rev	AGTGTAGCCCAAGATGCCCTTCAG
HPRT fw	Qiagen QT00166768
HPRT rev	Qiagen QT00166768
5' cutoff fw	CAGGATAATGTTCTCTTTGGGG
MyoD mRNAfw	CAGGTCTCAGGTGTAACAGGT
MyoD mRNA rev	TTTTGTTGCACTACACAGCAT

Rluc mRNA fw	AGACAAGATCAAGGCCATCG
Rluc mRNA rev	ACCATTTTCTCGCCCTCTTC
Fluc mRNA fw	ACTCTAAGACCACTACCAG
Fluc mRNA rev	GTAGACCCAGAGCTGTTTCATG
<b>Templates for in vitro transcription</b>	
T7 MD1-133b fw	TAATACGACTCACTATAGGGTTGGACAAGTGGTGCTCAAACCTC
MD1-133b rev	TGTGAACTTGGGCTTTCTCC
133b-SL rev	CCAGCATTACTTTTCATAAGC
T7 MD1 3' fw	TAATACGACTCACTATAGGGAAGTTGAGCCAAGGTTAGACCAG
MD1 3' rev	GATGTAGAATGTCACGGCGAAC
T7 MD1 5' fw	TAATACGACTCACTATAGGGCTCTTTGCAGTGGGACAGCTG
MD1 5' rev	GGACAAGTTGCAGGCAGGTCCC
T7 MYOD 3'UTR fw	TAATACGACTCACTATAGGGACACTCTTCCCAACTGTCC
MYOD 3'UTR rev	GCACTACACAGCATGCCT
T7 MD antisense A rev	TAATACGACTCACTATAGGGCTGCAGCCGTGTTTCATTCTCTG
MD antisense A fw	CATGCAGCATAACATTCATCCTAG
T7 MD antisense B rev	TAATACGACTCACTATAGGGCCATTTACTGGTGAAGAAGCAAC
MD antisense B fw	GTACACTGAGACTAAAGTACAC
T7 pri-miR-9-2 fw	Morlando et al., 2012
pri-miR-9-2 rev	Morlando et al., 2012
<b>Plasmid construction</b>	
MD1ΔHuR fw	TGGTGGAGAAAGAGAAGAGAAG

MD1ΔHuR rev	GCCGAGCTTTGCCAGCCCTGCTG
-------------	-------------------------

**Table S3, related to Figure 3. Small RNA seq analysis of scramble and HuR siRNAs-treated C<sub>2</sub>C<sub>12</sub> cells (2 days differentiation), available in download as an excel spreadsheet.**

In the summary page a description of the RNAseq data is available. Length, number and sequence of reads are reported together with miRNA name for each of the four lanes (A1-4). A 1,2 lanes correspond to scramble siRNA-treated cells, A 3,4 to HuR siRNA-treated cells. miR-133 a and b reads are reported separately.

## Extended experimental procedures

### microRNA binding predictions

miR-133 and miR-135 target predictions were performed using the miRanda algorithm, setting all the parameters to the default values. Results were then filtered for expression in muscle tissue according to the Gene Expression Barcode dataset: consensus proportion was set to 95% of the samples for the tissue named “Skeletal Muscle: Normal” in the Mouse\_4302 platform. The best 20 filtered targets of miR-133 and miR-135, ranked for the miRanda score, were reported in Table S1.

**Luciferase constructs and assays:** 3'UTR of HuR was amplified from mouse genomic DNA by polymerase chain reaction (PCR) with the oligos listed in table S2 and then cloned in NotI restriction site of the psicheck2 plasmid (Promega), downstream from the renilla luciferase (RLuc) gene. The same plasmid also contains the firefly luciferase (FLuc) to normalize transfection efficiency. The mutant derivative lacking the two miR-133 MREs was obtained by inverse PCR with the oligo listed in supplementary table 2. RLuc and FLuc activities were measured by Dual Glo luciferase assay (Promega).

**Plasmid construction:** The pMD1, p133 and p135 plasmids used in this work correspond to pMD1-ΔDrosha, pmiR-133a/b and pmiR-135a/b (pooled) described in Cesana et al. (2011) respectively. The pMD1ΔHuR plasmid, carrying the mutation in the HuR putative binding site, was generated by reverse PCR on pMD1-ΔDrosha using the oligonucleotides described in Table S2. pHuR was produced by cloning HuR cDNA into a pcDNA 3.1 (+) vector (Invitrogen).

**Drosha in vitro processing:** In vitro processing assay was carried out as previously described (Lee and Kim, 2007). Pri-miRNA substrates were prepared by in vitro transcription, using T7 RNA polymerase (Promega), from PCR amplified templates (oligonucleotides are listed in Table S2), in the presence of [ $\alpha$ -<sup>32</sup>P]UTP (Perkin-elmer). 40'000 cpm of each pri-miRNA transcript were incubated with 15  $\mu$ g of C<sub>2</sub>C<sub>12</sub> nuclear extract cells at 37°C for 90 minutes.

**Small RNA sequencing:** miRNA libraries were constructed and sequenced by the Illumina Cluster Station and HiSeq-2000 (Illumina Inc, CA, USA) at Beijing Genomics Institute at Shenzhen according to the manufacturer's protocol. Reads were aligned to mouse miRNA sequences present in miRBase (GRCm38). miRNA reads are available as a separate spreadsheet named “smallRNAseq”.

## Supplemental References

Kozomara A, Griffiths-Jones S. (2011) miRBase: integrating microRNA annotation and deep-

sequencing data. NAR 39 (Database Issue): D152-D157.